Pharmaceutical Research, Vol. 25, No. 3, March 2008 (© 2007)
DOI: 10.1007/s11095-007-9480-4

Research Paper

A Biodegradable pH-sensitive Micelle System for Targeting Acidic Solid Tumors

Vijay A. Sethuraman,[1] Myung Cheon Lee,[2] and You Han Bae[1,3]

Received August 14, 2007; accepted October 15, 2007; published online November 13, 2007

Abstract. A new pH-sensitive micelle delivery system based on TAT cell penetrating peptide and biodegradable sulfonamide grafted disulfide polymer is presented. The system consists of two components: (1) A polymeric micelle made of Poly(L-lactic acid)-*b*-poly(ethylene glycol) (PLLA-*b*-PEG) conjugated to TAT (TAT-micelle), (2) A pH-sensitive diblock copolymer (poly(L-cystine bisamide-*g*-sulfadiazine))-*b*-PEG (PCBS-*b*-PEG). The anionic PCBS complexed with cationic TAT of TAT-micelles forms the final carrier. PCBS showed rapid degradation in the presence of cysteine. The TAT-micelles showed increase in particle size between pH 8.0 and 7.0 upon mixing with PCBS-*b*-PEG indicating complexation. As the pH was further decreased (pH 6.8 to 6.0) two populations were observed, one of normal TAT-micelles and the other of aggregated PCBS-*b*-PEG. Flow cytometry showed significantly higher uptake of TAT-micelles at pH 6.6 indicating deshielding compared to pH 7.4. The anticancer drug doxorubicin (DOX) was encapsulated into the TAT-micelles, and the *in vitro* cytotoxicity at different pHs was evaluated. The system was able to distinguish pHs 7.2 and 7.0 in terms of cytotoxicity.

KEY WORDS: degradable pH sensitive polymer; disulfide polymer; pH-sensitive polymer; tumor pH.

INTRODUCTION

Biodegradable pH-responsive drug carriers have the potential not only to provide selective drug release at specific targets like tumors, but also to be rapidly cleared or degraded in the body after delivering the cargo. In recent years, pH-sensitive polymeric carriers in various forms of micelles (1,2), vesicles (3,4), and nanoparticles (5,6) have seen rapid development. Particularly, polymeric micelles are being extensively studied as a promising nanoscale drug carrier since the pioneering work in early 1990s (7). Polymeric micelles have many advantages such as small size (10 to 200 nm) for passive accumulation in solid tumors by 'enhanced permeation and retention' (EPR), improved stability, biodegradability and high flexibility for structural and chemical modifications (8,9).

Early generation polymeric micelles simply accumulated on the tumor extra cellular matrix (ECM) and did not provide high enough concentrations of anticancer drugs to kill the tumors, because most cytotoxic drugs act inside the cells and not on the ECM (10,11). Therefore, tumor targeting carriers have been modified such that they accumulate by the EPR effect on tumor cells followed by active internalization into tumor cells (12). Such improved active targeting technology is being developed by using binding characteristics between tumor specific antigens and their monoclonal antibodies (mAb) (13), binding fragments specific to a tumor associated surface antigens (14), or between ligands and their corresponding receptors (15). Such active targeting carriers show enhanced capability to translocate the micelles into tumor cells (16).

In most cases, the therapeutic drugs are released from the polymer scaffold in the lysosomal environment and cleaved by enzymatic degradation or pH-sensitive hydrolysis (17). Even after drug is released from the carrier, the diffusion through the lysosomal membrane to cytosol and then to the nucleus, has proved to be a formidable barrier (18). TAT-mediated cytoplasmic uptake of drug conjugates can deliver the cargo directly at periphery of the nucleus avoiding the endocytotic pathway (19,20). The probable mechanism of internalization of TAT (Trans-Activator of Transcription) peptide is via electrostatic interaction and hydrogen bonding or macropinocytosis depending on the size of the cargo (21). A major hurdle in using TAT in the body is its non-specificity, since it can interact with any cells.

It has been firmly established that the pH of ECM of most solid tumors is relatively lower (pH<7.0) than that of normal tissues (22,23). The lower pH comes from the high metabolic rate of tumor cells which leads to production of excess lactic acid and hydrolysis of ATP under hypoxic conditions (22). This difference in pH between tumor and normal cells, even

[1] Department of Pharmaceutics and Pharmaceutical Chemistry, University of Utah, 421 Wakara Way, Suite 318, Salt Lake City, Utah 84108, USA.
[2] Department of Chemical and Biochemical Engineering, Dongguk University, 3-26 Pil-dong, Choong gu, Seoul 100-715, South Korea.
[3] To whom correspondence should be addressed. (e-mail: you.bae@utah.edu)

though very small, has instigated many investigators to develop pH-sensitive drug carriers (1,24,25) that use it as a trigger. Among these, drug carriers having sulfonamide pendant groups are most promising as they have shown sharp transition ranges around physiological pH (20,26–28).

In our previous work (16), we constructed a 'smart micellar nanoplatform' drug delivery system that could possibly hide the non-specific TAT peptide in the blood and expose it at tumor ECM. The delivery system was prepared by integration of two components: (1) chemotherapeutic polymeric micelle—consisting of poly(ethylene glycol) (PEG) outer shell, with TAT attached to the PEG and a hydrophobic core made of poly(L-lactic acid) into which any chemotherapeutic could be incorporated; (2) the TAT shield—an ultra pH-sensitive smart block copolymer PSD (polysulfonamide)-*b*-PEG. When the polymer was mixed with the TAT micelle, the positively charged TAT peptide was shielded by the negatively charged PSD of the PSD-*b*-PEG block copolymer.

The main drawback of above system is that the 'shield' PSD-*b*-PEG is non bio-degradable. There is a strong possibility that the polymer may cause toxic effects if its accumulated dosage increases above a critical point. In this work, we delineate a new biodegradable-TAT shield—an ultra pH-sensitive smart block copolymer PCBS-*b*-PEG, (poly(L-cystine bisamide-*g*-sulfadiazine)) instead of PSD-*b*-PEG. It was applied to the same inner carrier system (TAT-PEG-PLLA-drug). A model of the proposed drug delivery system is shown in Fig. 1.

MATERIALS AND METHODS

Materials

Sulfadiazine [4-amino-*N*-(2,6-dimethoxy-4pyrimidynyl)-benzenesulfonamide] (SA), *N*-hydroxysuccinimide (HOSu) and dicyclohexyl carbodiimide (DCC) were purchased from Aldrich Chemical Co. (Milwaukee, WI, USA) and used without further purification. ^{1}H NMR spectra were acquired on a Varian INOVA 400 at 400 MHz at 25°C. Molecular weight was determined by size exclusion chromatography (SEC) on an AKTA FPLC system with a Superose 12 column equipped with UV and refractive index detectors (Amersham Biosciences Corp., Piscataway, NJ, USA), calibrated with poly[*N*-(2-hydroxypropyl)methacrylamide] (HPMA) standards with a molecular weight range of 2 to 120 kDa. FITC labeled TAT peptide was synthesized at the DNA/Peptide Core Facility at the University of Utah (Salt Lake City, UT, USA). All other chemicals were of reagent grade and were used without further purification.

Synthesis of Biodegradable PCBS-*b*-PEG

The synthesis of biodegradable PCBS-*b*-PEG is outlined in Scheme 1. The synthesis involved three steps. First L-Cystine bisamide polymer was synthesized from L-cystine and EDTA-Dianhydride. This polymer was then conjugated to PEG. Finally sulfadiazine was grafted on to L-Cystine bisamide part of the copolymer.

Synthesis of L-Cystine Bisamide Polymer (PCB). L-Cystine was reacted with EDTA (ethylene diamine tetra acetic acid) dianhydride in carbonate buffer (pH 9.0) at room temperature for 18 h. The product was then dialyzed using a regenerated cellulose membrane (M.W cutoff 3,500 kDa) against water for 3 days to remove any unreacted monomers and salts. The product was then freeze dried to obtain the final polymer. The polymer was analyzed with NMR and molecular weight was determined with size exclusion chromatography (SEC). All the SECs were performed on an AKTA FPLC system with a Superose 12 (10/300 GL) column and UV and refractive index detectors. The molecular weights were calibrated with poly[*N*-(2-hydroxypropyl)methacrylamide] standards. The NMR spectra (not described here) were similar to that of Zong *et al.* (29) whose polymers have similar backbone structure.

Conjugation of L-Cystine Bisamide Polymer with PEG (PCB-b-PEG). The methyl carboxy PEG 5 kDa was coupled with the L-Cystine polymer using *N*,*N*′-Dicyclohexylcarbodiimide (DCC) and *N*-Hydroxysuccinimide (HOSu) as the coupling agents. First PEG was activated in tetrahydrofuran (THF) by HOSu with a molar ratio of PEG:HOSu:DCC=1:2:2. The reaction was continued for 1 h after which DCC was added and the mixture was allowed to react for 15 h. Two to three drops of water was added to precipitate out DCU. The DCU was filtered and the filtrate was poured into tenfold *n*-hexanes for precipitation of the activated PEG. The activated PEG was then coupled with the terminal amine of PCB using DMSO as a solvent. This method ensured that the amine group reacted only with the COOH of PEG and not with other COOHs present in PCB. The conjugation was confirmed by using NMR and SEC.

Attachment of Sulfadiazine to L-Cystine bisamide of the copolymer (PCBS-b-PEG). PCB-*b*-PEG was first dissolved in 2:3 mixture of water and DMSO and reacted with DCC and HOSu overnight at room temperature to activate the carboxylic groups in PCB. The reaction mixture was then filtered to remove the by product DCU and dialyzed against water to remove the unreacted impurities. The product was vacuum dried for 2 days to remove all the solvents. This product was then reacted with sulfadiazine in 0.01 N NaOH for 8 h at room temperature to yield the final polymer. The polymer was analyzed with NMR and IR spectroscopy and the amount of sulfadiazine attached was determined by measuring the absorbance at 270 nm and comparing it with a standard curve.

In Vitro Degradation of Biodegradable Polymers

The degradation of each copolymer was studied in the presence of L-cysteine at 15 mM (equivalent to free thiol concentration in the plasma). Two systems were evaluated: (1) PCBS polymer by itself and (2) PCBS complexed with positively charged PEI. The copolymers (420 mM, monomeric repeat unit concentration) were incubated with 15 mM L-cysteine in PBS (pH 7.4) at 37°C. The molecular weight distributions were evaluated at different time intervals by SEC. Before injection into the SEC column, the PEI was separated from PCBS by diluting the mixture into two times volume of 0.5 M NaCl solution. The reduction in molecular weight of copolymers after the incubation was calculated as the percentage of the weight-average molecular weight of the remaining copolymers at various time points of the incubation to their original values.

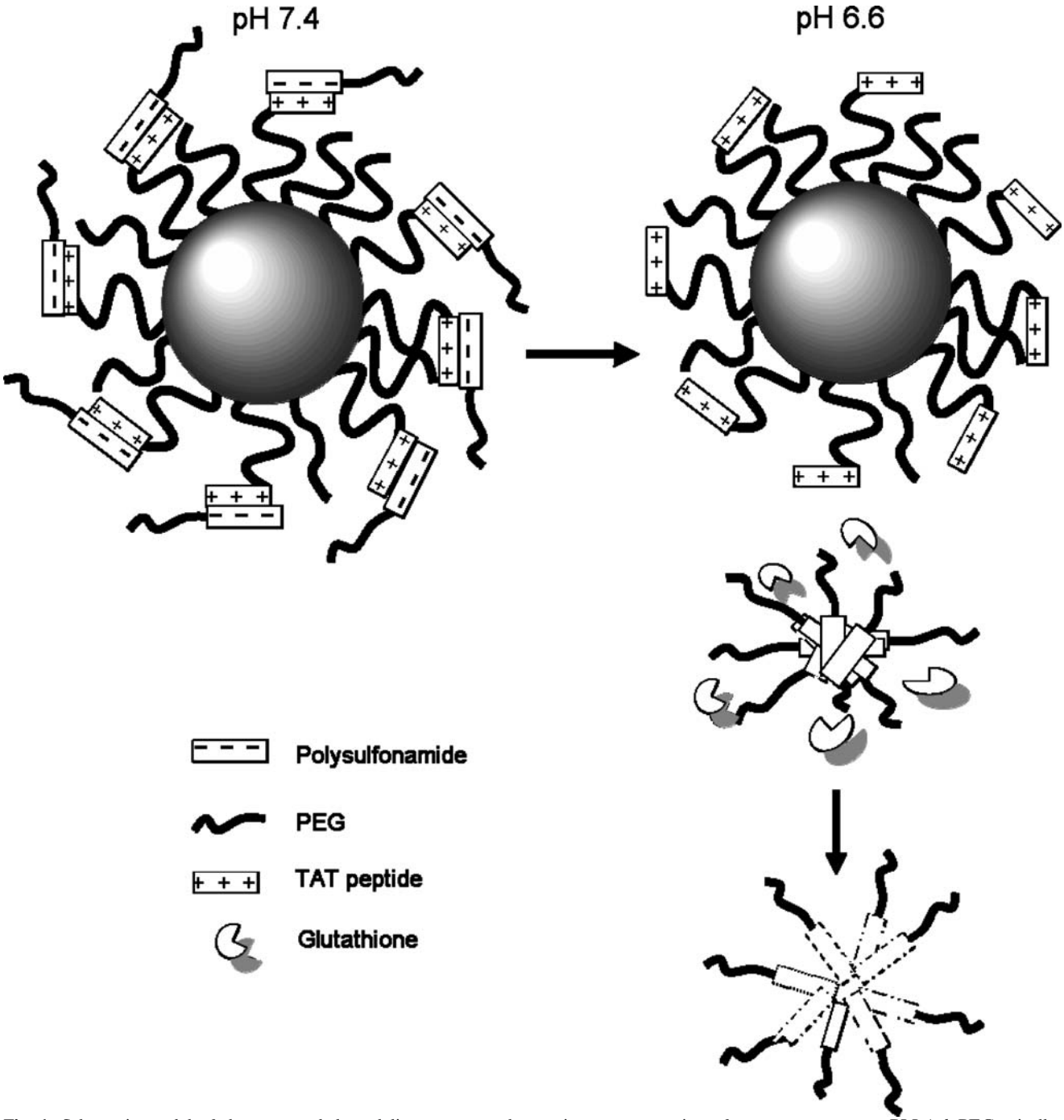

Fig. 1. Schematic model of the proposed drug delivery system: the carrier system consists of two components, a PLLA-*b*-PEG micelle conjugated to TAT and a pH sensitive diblock polymer PCBS-*b*-PEG. At normal blood pH (pH 7.4), the sulfadiazine is negatively charged, and when mixed the TAT-micelle, shields the TAT by electrostatic interaction. Only PEG is exposed to the outside which could make the carrier long circulating; when the system experiences a decrease in pH (near tumor pH 6.6) sulfonamide will lose charge and detach, thus exposing TAT for interaction with tumor cells; the detached PCBS polymer is degraded rapidly by the native glutathione.

pH-sensitivity Studies of PCBS-*b*-PEG Using Light Transmittance

Fifteen milligrams of various M.Ws. PCBS-*b*-PEG was dissolved in 2 ml 0.1 N NaOH solution and titrated against 0.1 N HCl. The optical transmittance of the solution after each HCl addition was measured. The transmittance was measured at 500 nm using a Varian Cary 1E UV/Vis spectrometer. The transmittances at different pHs were expressed as percentage relative to the transmittance at pH 12.0.

Synthesis of Micelle Components PLLA-*b*-PEG and PLLA-*b*-PEGmal

The block copolymer was synthesized using standard ring opening polymerization of L-Lactide and mono hydroxy

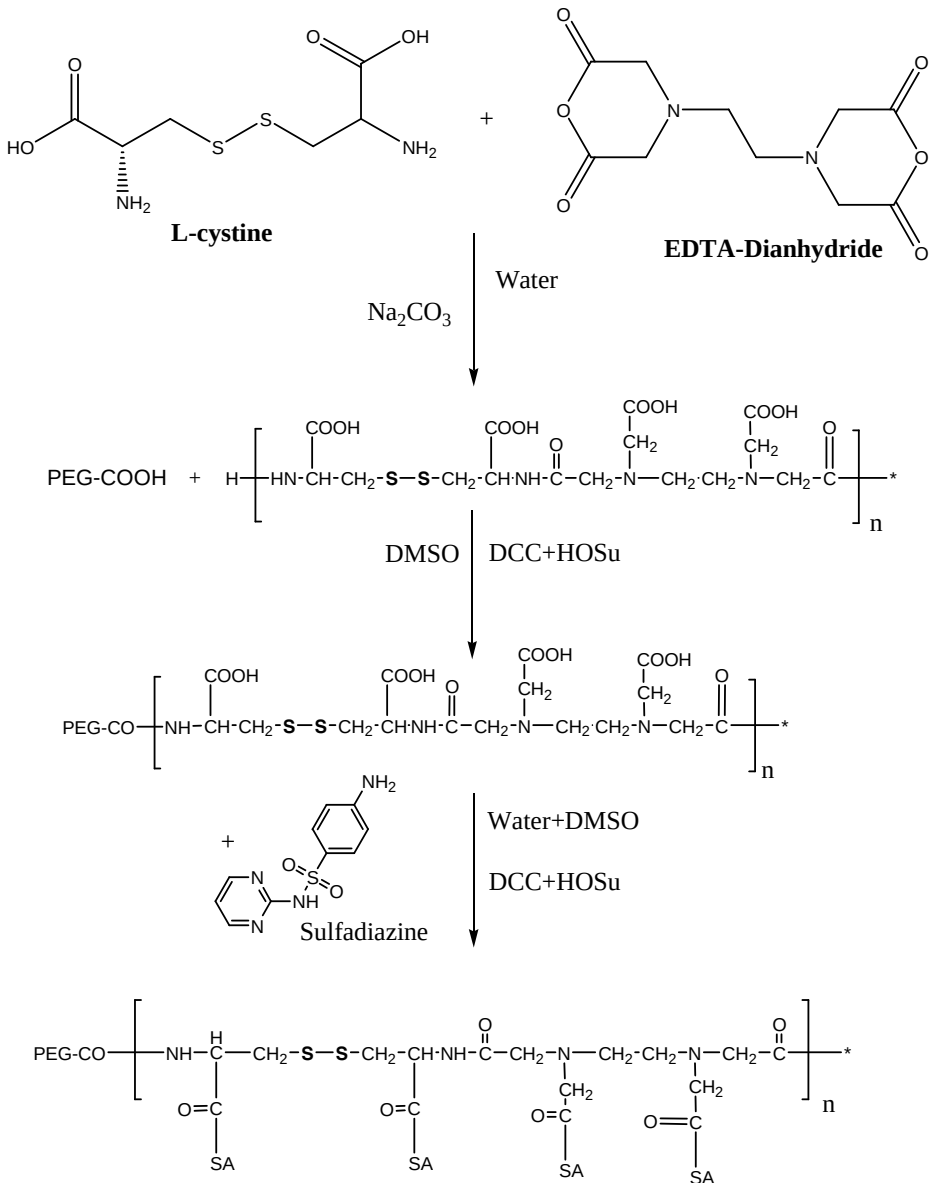

Scheme 1. Synthesis scheme of PCBS-*b*-PEG from L-cystine and EDTA-Dianhydride.

PEG with stannous octoate as catalyst (30). First, to remove any traces of water, the starting materials (2.5 mmol of poly(ethylene glycol)-monomethyl ether 5 kDa and 70 mmol of L-lactide) were each dissolved in 150 ml toluene separately in round-bottomed flasks. Thirty milliliters of toluene was distilled off using a water separator at 120°C under nitrogen atmosphere. The water-free solutions were united in a three-neck flask and a precisely weighed amount of 100 mg stannous 2-ethylhexanoate (1 wt.% of L-lactide) was added and then the mixture was refluxed for 24 h under nitrogen atmosphere at 110°C. Upon completion of the reaction, the mixture was precipitated in tenfold ice cold ethyl ether. The precipitated polymer was then filtered with an aspirator and dried in a desiccator at room temperature at a pressure of less than 0.1 mbar using a RV5 two stage vacuum pump (Edwards, Crawley, West Sussex, UK). After drying for 3 days, the polymer was ground under liquid nitrogen in a mortar to obtain a free flowing powder. The molecular weight and composition of the final polymer was determined using ^{1}H-NMR spectroscopy (31).

A similar procedure was employed to synthesize PLLA-*b*-PEGmal. Poly(ethylene glycol)–maleimide ether was used instead of poly(ethylene glycol)–mono methyl ether as the starting material and was purchased directly from Nektar Therapeutics Inc. (San Carlos, CA). The maleimide group on the PEG was used to conjugate with the TAT peptide via a thio-ether linkage.

Preparation of Polymeric Micelles

The polymeric micelles were formed by using diafiltration method. PLLA-*b*-PEGmal was dissolved in dioxane and PLLA-*b*-PEG was dissolved in DMSO. PLLA-*b*-PEGmal solution (2 wt.%) was mixed with PLLA-*b*-PEG solution and dialyzed in phosphate buffer saline (0.1 M PBS) for 3 days. To form micelles and remove the organic solvents the PBS was changed every 1 h for the first 6 h and then once every 8 h after that. The initial concentration of the polymers in the organic solvents was adjusted such that the final concentration of polymer in the micelle was approximately 1 g/l. The

micelles were stable in aqueous solution for over 1 month (stored at 4°C). The stability was measured by determining if there was any change in particle size of the micelles with time using dynamice light scattering with Malvern Zetasizer 3000 HS (Malvern Instruments, Worcestershire, UK). The solutions were subsequently lyophilized after filtering through a 0.8 μm syringe filter. The yield (69.3 wt.%) of micelles was calculated by weighing the freeze-dried micelle powder.

Conjugation of TAT to Polymeric Micelles to Form TAT-Micelles

The TAT peptide [FITC-Gly-Cys-$(Gly)_3$-Tyr-Gly-Arg-$(Lys)_2$-$(Arg)_2$-Gln-$(Arg)_3$] was conjugated to the maleimide on the PEG of the micelles via a thio-ether linkage. The polymeric micelles in PBS, having maleimide groups on the outside of the shell, were mixed with a slight molar excess of TAT peptide solution at pH of 7.2 under nitrogen atmosphere. The reaction mixture was stirred overnight in the dark at room temperature. The TAT conjugated micelles were then separated from unreacted TAT by using a PD10 column in PBS. The various fractions obtained were analyzed with HPLC and fluorescence spectroscopy to confirm conjugation and purity of product. The analyses showed 96% TAT conjugated to the micelles and about 4% free TAT. Our previous findings (32) showed that 2% TAT conjugation showed good internalization and other micelle properties. Throughout these studies 2% TAT conjugated micelles were used

Doxorubicin Loading into TAT-micelles

Doxorubicin HCl (DOX.HCl) at 2 mg/ml concentration was (10 ml) stirred with twice the number of moles of TEA in DMSO overnight to obtain the DOX free base. The TAT-micelle was lyophilized to solid powder form. Fifty milligrams of this powder was then dissolved in DMSO and stirred along with DOX base for 3 h. The solution mixture was then transferred into a pre swollen dialysis membrane having 3.5 kDa MW cutoff. Dialysis was then carried out against PBS buffer at pH 7.4 for 1 day with exchange of medium several times. The amount of DOX loaded was determined by first lyophilizing the DOX loaded TAT-micelles and then dissolving the powder in DMSO and measuring the absorbance of the solution at 481 nm and comparing with a standard curve prepared with DMSO. The drug loading efficiency the micelles was 62% by weight. The final DOX concentration of DOX used in all the studies was 1 mg/ml.

Particle Size and Zeta Potential Determination of Various Micelles

Zeta potential and particle size were measured using laser light scattering technique on a Malvern Zetasizer 3000 HS (Malvern Instruments, Worcestershire, UK) equipped with He–Ne laser (633 nm). The PMC (polymer-micelles complexes: PCBS-*b*-PEG complexed with TAT-micelle) were formed by mixing the two components together at individual pHs having 10 mM NaCl. The dynamic light scattering data was fitted with intensity average Gausian distribution.

Flow Cytometry Studies

Human breast adenocarcinoma (MCF-7) cells were obtained from the Korean Cell Line Bank (KCLB, Seoul, Korea). They were maintained in RPMI-1640 medium with 2 mM L-glutamine, 1% bovine insulin, 1% penicillin–streptomycin and 10% fetal bovine serum in a humidified incubator at 37°C and 5%CO_2 atmosphere.

The cells (5×10^4 cells/ml) grown as a monolayer were harvested with 0.25% (w/v) trypsin–0.03% (w/v) EDTA solution and were seeded in 12 well plates at a density of 2.5×10^5 cells per well and incubated for 24 h. Medium with serum was replaced with 1 ml serum free media with either pH 6.6 or 7.4, 1 h before addition of various complexes. The test samples TAT-micelles and PMC prepared at pH 7.4, were added (2% TAT on the surface of the micelles and 20 μl of 0.780 mg/ml micelles, concentration about four times the CMC of the micelles) into the cell wells and incubated for 30 and 60 min. The incubation solution was then removed and the cells were washed with 20 mM PBS. The cells on the surface of the plate were detached using trypsin solution and then fixed with 2.5% glutaraldehyde before flow cytometry analysis. The fluorescence of the TAT-micelles internalized into the cells was measured by using FACSCAN flow cytometer (Becton Dickinson Inc., USA). The excitation wavelength was set at 488 nm and measured with the FL1 channel.

Cytotoxicity of DOX Loaded Micelles

MCF-7 harvested from growing cells as a monolayer were seeded in a 96-well plate in 200 μl of RPMI 1640 medium 24 h prior to the cytotoxicity test. Free DOX, DOX loaded TAT-micelles and DOX loaded PMC were prepared in RPMI 1640 medium at various pHs using 0.01N NaOH or 0.01N HCl) immediately before use as described in a previous report (1). The DOX and DOX-equivalent concentration of 10 μg/ml was added to the medium-removed 96-well plate and incubated for 48 h. Chemosensitivity was assessed using tetrazolium salt MTT assay. PBS (100 μl, pH 7.4) containing 20 μl of MTT (500 μg/l) solution was added to each well. The plate was incubated for an additional 4 h, and then 100 μl of DMSO was added to each well. The absorbance of each well was read on a microplate reader using a test wavelength of 570 nm and a reference wavelength 630 nm.

Statistical Analysis

All experiments were repeated at least three times with a minimum sample size of three. Student's *t* test was used, using STATA statistical software (StataCorp LP, Texas), to test for statistical difference between samples. Comparisons having p value ≤ 0.05 were considered significant.

RESULTS AND DISCUSSION

Synthesis of PCBS-*b*-PEG Copolymers

A new biodegradable pH-sensitive polymer that is capable of shielding TAT peptide at physiological pH and deshielding at tumor pH has been explored in this manuscript. First L-Cystine bisamide polymer (PCB) was synthe-

sized by condensation copolymerization of L-Cystine and EDTA dianhydride (Scheme 1). After that PEG 5 kDa was conjugated to the polymer. As the final step sulfadiazine was grafted to the PCS polymer to obtain the final polymer. The synthesis conditions and physicochemical properties are listed in Table I. The carbonate buffered media resulted in polymers of high yield and optimum molecular weight for pH sensitivity compared to water and Na_2CO_3. This was because the water system was not able to maintain the pH at 8.0 with the progress of polymerization, but on the other hand the carbonate buffer was able to maintain the pH at 8.0. This helped maintain a narrow molecular distribution and produced desired molecular weights and better yields.

In Vitro Degradation of Copolymers

Figure 2 (N=3, mean±SD) shows the molecular weight reduction of the polymeric ligands from their original values at various time points in the incubation with 15 mM cysteine in 10 mM PBS (pH 7.4) at 37°C. The disulfide-thiol exchange reaction between the polydisulfide backbone and cysteine results in molecular weight decreases with increasing incubation time.

In this experiment PEI was used rather than TAT-micelles mainly because PEI is much cheaper compared to TAT peptide and complexity of the experiment is greatly reduce. The rates of molecular weight reduction were rapid in the case of PCBS 23.2 kDa and relatively slow for the PCBS-PEI complex. The PCBS polymer completely degraded into low molecular weight species within 8 h but the PCBS-PEI complex degraded only 30%. The PCBS polymer shows degradation similar to the disulfide polymers reported by Kaneshiro *et al*. (33). It is also seen that the PCBS polymer is stable in plain PBS and shows only slight degradation in the presence of BSA protein. This degradation may be due the disulfide cleavage by the exposed cystine amino acid in BSA.

The PCBS-PEI complex is formed by charge-charge interaction between negatively charged sulfadiazine (pKa=6.48) in PCBS and positively charged PEI. Due to this interaction the polymers condense to form nanoparticles (as shown in our previous work (34)).It is hypothesized that only a small percentage of the disulfide backbone is exposed to the disulfide-thiol exchange reaction. As the outer exposed disulfide backbones degrade they in turn are able to attack the inner layers of the complex and degrade them. So the degradation is slow until 240 min (degradation of only the exposed backbone) after which the degradation is relatively rapid because of attack on the inner layer disulfide bonds by outer layer thiols formed, analogous to autocatalysis. This could possibly mean that when the carrier system is injected into the body the PCBS maintains its integrity during circulation (initial times) and may degrade upon extravasation (after 240 min).

pH-sensitivity of Various PCBS-*b*-PEG Polymers

The pH response of different molecular weights of PCBS-*b*-PEG was examined by preparing the polymer solutions in 0.1 N NaOH and measuring their turbidity by titrating against 0.1 N HCl. Figure 3 shows the pH-dependent turbidity profiles of three different molecular weights. It is clearly seen that they all show very sharp pH transitions and that the transition pH increases with increase in molecular weight and mole percent of SA in the copolymer. The pH-dependent solubility was reversible and no hysteresis was observed in the ionization/deionization process. PCBS11.3k-*b*-PEG5k shows the transition, from being in solution phase to forming aggregates or self assembled micelles between pHs 6.7 and 6.4 (Fig. 3a) whereas PCBS23k-*b*-PEG5k shows transition between pHs 7.0 and 6.7 and PCBS42k-*b*-PEG5k has transition from pH 7.3 to 6.9. The formation of aggregates or micelles mainly depended on the concentration of PCBS-*b*-PEG used. The higher concentrations usually formed aggregates (>2 mg/ml) while lower concentrations formed micelles.

The transition point of PCBS-*b*-PEG shifts to higher pH with increase in molecular weight mainly due to the neighboring group effect on the sulfadiazines. The amount of sulfadiazine conjugated (Table I) also contributes to the difference in transition points (35). The precipitation of the copolymers may occur at a critical composition of ionized and unionized PCBS. The polymer solubility transition occurs at a critical balance of chain hydrophilicity/hydrophobicity, thus allowing the transition at almost constant content of the unionized form. At higher SA content, a higher degree of ionization is required for solubility, while at a lower content only a few fractions will cause solubilization.

The carboxylic acid based polymers show transitions in about one pH unit which is very broad, and even that transition is much below the physiological and tumor pH range making them less attractive for physiological applications. The PCBS-*b*-PEG polymer , on the other hand, shows transition within 0.2 pH units in between the physiological and tumor pH (34). The sulfonamide group is readily ionizable at high pH because the strong electronegativity of the oxygen atoms of the sulfonyl group draws electrons from the

Table I. Synthesis Conditions and Physicochemical Characterization of PCBS-*b*-PEG

Polymer PCB						PCBS-*b*-PEG
Feed ratio L-Cys:EDTA.da	Water	Na_2CO_3(g)	Mn (kDa)	Mw (kDa)	Yield (%)	SA attached (%)
1:1.1	30	4.2	10.8	22.4	52	65
1:1.1	20	4.2	11.3	25.7	65	75
1:1	24	2.4	43.3	63.4	74	91
1:1		24 ml carbonate	23.2	29.6	81	97
1:1		Buffer	25.7	32.4	80	94

L-CYS L-Cystine, *EDTA.da* EDTA-Dianhydride.
Apparent Mn and Mw were determined using size exclusion chromatography and the SA contend was determined by UV spectroscopy at 270 nm.

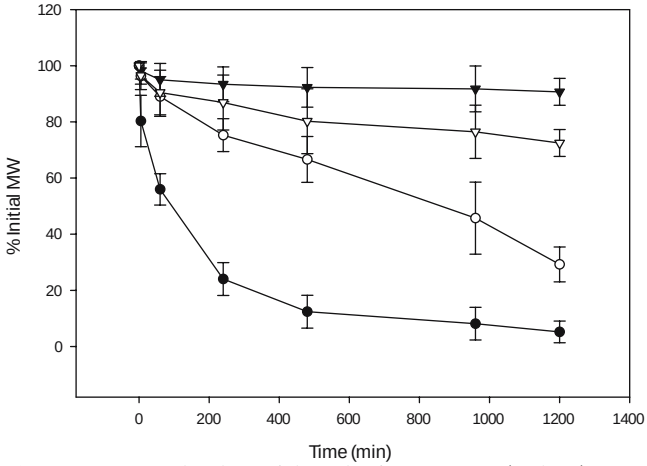

Fig. 2. Percent molecular weight reduction of PCBS (23 kDa) upon incubation at 37°C with (*filled inverted triangle*) PBS buffer, (*open inverted triangle*) 2 mg/ml BSA protein and (*filled circle*) 15 mM cysteine in PBS at varying incubation time (in minutes). (*open circle*) Degradation of PCBS shielded with 25 kDa PEI. Molecular weight as determined by size exclusion chromatography (SEC) (N=3, mean ± SD).

sulfur atom, which in turn pulls the electrons from the nitrogen atom (Fig. 3b) (34,36,37). This results in nitrogen pulling electrons from the N–H bond and thus releasing the proton. The pKa of the sulfonamide compound is governed the by diazine group, which is an electron-withdrawing group. The

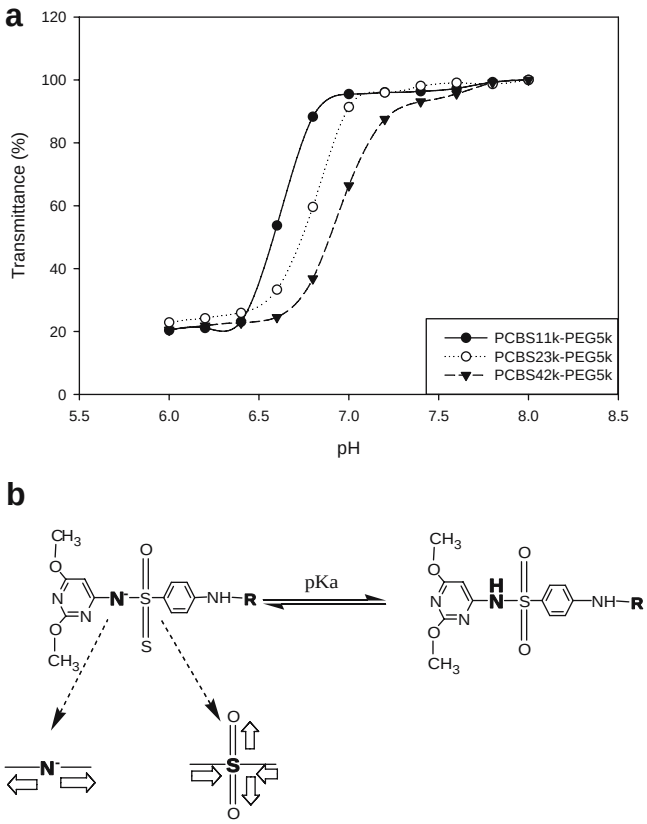

Fig. 3. a, **b** pH response of polymer PCBS-*b*-PEG [n=3]: The transition pH is governed by the molecular weight of the polymer and amount of sulfonamide attached.

PCBS23k-*b*-PEG5k was chosen for further studies because of its optimal pH transition between normal pH and tumor pH.

TAT-micelles Shielding/Deshielding by PCBS-*b*-PEG as a Function of pH

TAT-micelles of PLLA12k-*b*-PEG5k polymer with 2% TAT conjugation were used throughout the studies as these were well characterized in our previous report (16). The TAT-micelles, after complexation with pH sensitive PCBS23k-*b*-PEG5k, showed a slight increase in size between pHs 8.0 and 7.0 (60–100 nm) indicating complexation (Fig. 4a). The increase in size may be due to attachment of the copolymer and reduction in surface charge of the micelles.

Between pH 6.8 to 6.0 two populations were observed, one about 50 nm in size that corresponds to TAT-micelles (16) and the other about 325 nm. The larger particles, is

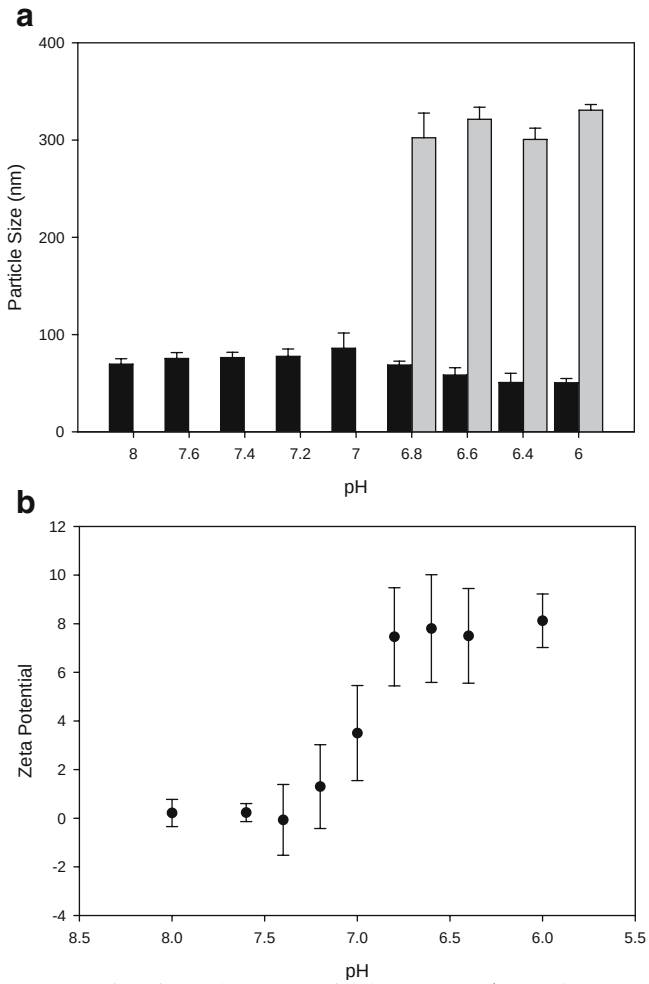

Fig. 4. Particle size and zeta potential data of PMC (PCBS-*b*-PEG + TAT-micelles complex) at various pHs. **a** Particle size of the complexes from pH 8.0 to 6.0. From pH 8.0 to 7.0 unimodal particle distributions observed, indicating PCBS-*b*-PEG complexed with the micelles, 6.8 to 6.0 shows bimodal particle distribution, the bigger population may be the aggregates of the neutral PCBS-*b*-PEG (N=3, mean ± SD). **b** Zeta potential studies indicate a similar trend, the particles show near zero zeta potential between pH 8.0 and 7.2 that indicate complete complexation and positive potential (of TAT, PCBS being neutral) from pH 6.8 to 6.0 indicating decomplexation (N=3, mean ± SD).

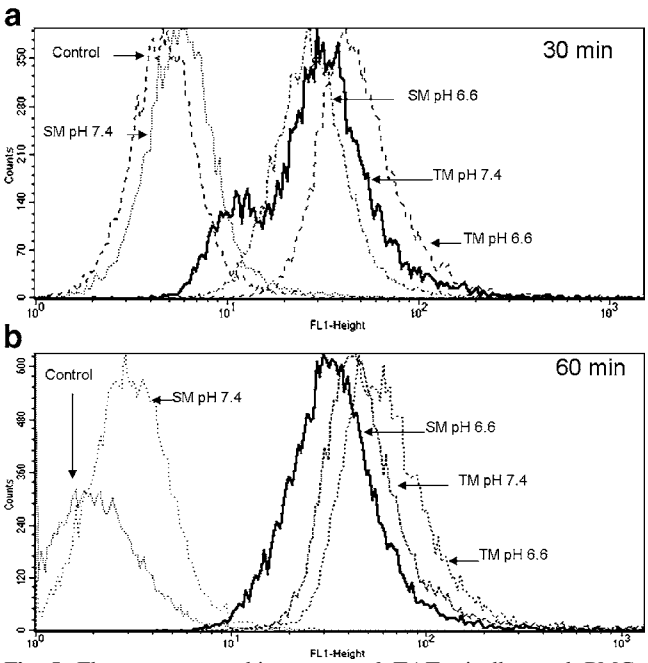

Fig. 5. Flow cytometry histograms of TAT-micelles and PMCs internalized into MCF-7 cells at pHs 7.4 and 6.6 at **a** min and **b** 60 min. (Control histograms are of cells incubated with plain micelles without TAT). SM = Shielded-micelles (PMCs); TM = TAT-micelles.

speculated to be the nanoparticles formed from the neutralized PCBS23k-*b*-PEG5k. Indeed we found that when PCBS23k-*b*-PEG5k was dissolved in NaOH and the pH was brought down to pH 6.8 and below the polymer formed nanoparticles of about 400 nm (data not shown). This strongly indicates that the larger particles in the bi-modal distribution of shielding/deshielding study may be the neutralized PCBS23k-*b*-PEG5k.

Zeta potential measurements showed a similar trend, substantiating the trend observed with particle size distribution. From pH 8.0 to 7.0 the zeta potential was around zero indicating complete shielding of TAT (TAT being positively charged) and from 6.8 to 6.0 the zeta potential was increased to 8.0 mV, which is the same as the zeta potential measured for the TAT-micelle alone (Fig. 4b), implicating the deshielded TAT. Even though the TAT peptide has a high positive charge, the zeta potential of the micelles is relatively low; this is attributed to the low surface density of TAT conjugated (2%) on the micelle surface.

There is a slight chance that the charge neutralized PCBS/TAT be buried in the micelle core at pH 7.4 or the uncharged PCBS part be buried at pH 6.6. The extent of this occurring is very slight due to the presence of PEG in PCBS and on the outer surface of the micelles. PEG, having a highly flexible backbone, being thermodynamically active and due to its large size, will minimize this from happening.

Internalization of TAT-micelles

The MCF-7 adenocarcinoma cell lines were used to test for the uptake of TAT-micelles and shielding/deshielding by PCBS23k-*b*-PEG5k. Figure 5 shows the flow cytometry data for various micelles taken up at 30 and 60 min. *x*-Axis represents the fluorescence intensity (FL-1, in logarithmic scale) and *y*-axis, the number of cells corresponding to that intensity. The TAT-micelles show similar histograms for both pHs 7.4 and 6.6 indicating that the pH does not affect internalization (Fig. 5a). It is seen that the TAT-micelles enter the cells very quickly as even at 30 min of incubation these micelles show higher FL-1 (fluorescence) reading than PMCs (shielded-micelles). The PMCs show marked difference in uptake between pH 7.4 and 6.6. The uptake is similar to that of control cells at pH 7.4, indication strong shielding (the FL-1 histogram is very close to that of control cells). At pH 6.6 the PMCs show uptake about one order of magnitude more than pH 7.4 indicating deshielding. Also the uptake at pH 6.6 is just slightly less than TAT-micelles (no significant difference) as the FL-1 histograms are very close to each other. A similar trend for PMCs is seen at 1 h incubation, with difference in histogram peaks between pHs 7.4 and 6.6 further away from each other than at 30 min. This indicates more uptake at 1 h than 30 min.

At pH 6.6 the PCBS of pH sensitive PCBS23k-*b*-PEG5k polymer becomes neutral and detaches from TAT of the micelles. Due to this detachment, the exposed TAT is able to interact with the cells and internalize into the attached micelles. The same shielded micelles at pH 7.4 on the other hand, show low uptake. This could be due to the fact that the pH sensitive negatively charged PCBS-*b*-PEG is still complexed with the positively charged TAT and is preventing it from interacting with the cells. Complete shielding is observed at pH 7.4; on the other hand the deshielding of the TAT-micelles at pH 6.6 is not total. The fluorescence for deshielded TAT-micelles is a little less than TAT-micelles. This may be due to various reasons: for instance, incomplete detachment of the sulfonamide groups from the TAT and/or hindrance by the separated PCBS-*b*-PEG on the surface of the cells.

The deshielded micelles have ten times more fluorescence than the shielded micelles (Fig. 5), which is indicated by the difference in peak positions over the *x*-axis. This

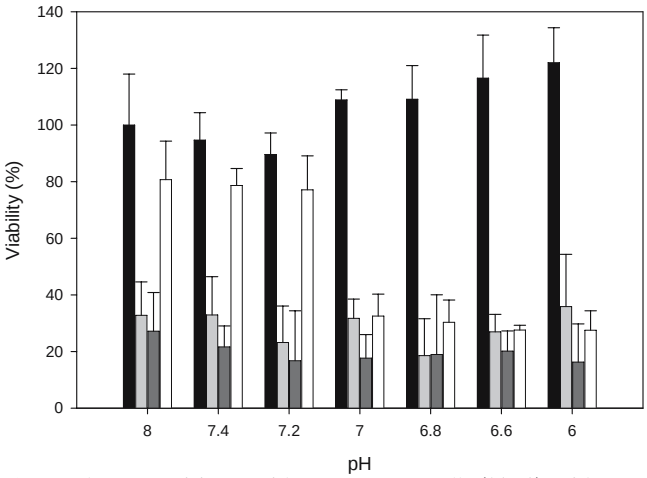

Fig. 6. The cytotoxicity of with no treatment cells (*black*), with free DOX (*light grey*) or with DOX loaded TAT-micelles (*dark grey*) and shielded-micelles (*white*) between pHs 8.0 and 6.0 after 48 h of incubation (N=7).

difference is an improvement in the efficiency of shielding/deshielding over our previous report (16). The shielding/deshielding of this carrier system is about 8 times better than our previous report. This has been accomplished by changing the type of sulfonamide from sulfadimethoxine (pKa=6.1) to sulfadiazine (pKa=6.4) and also by changing the molecular weight of the pH sensitive polymer.

In Vitro Cytotoxicity of DOX Loaded Micelles Against MCF-7 Cells

Figure 6 shows the cytotoxicity data of DOX loaded micelles against MCF-7 cells as a function of pH. As the pH was decreased from pH 8.0 to 6.0 the viability of cells without any treatment increased from 100% at pH 8.0 to 120% at pH 6.0 ($p<0.1$). It has been reported in literature that an acidic pH in the extra cellular matrix of cancer cells make them more aggressive and help them invade the neighboring healthy cells and metastasize (38). An increase in viability observed here supports this theory because the MCF-7 cells seem to grow better in acidic medium. Treatment with DOX shows a toxic effect as expected, but there is no significant difference in toxicity with varying pHs. Incubation with TAT-micelles shows more toxicity than free DOX; this could be because the TAT is able to take the DOX loaded micelles not only into the cells but also to the nucleus. DOX elicits apoptosis by interacting with the DNA inside the nucleus of the cells (39). TAT, being a strong nuclear localization agent may be able to move the micelles to the nucleus and hence elicit higher toxicity.

The shielded-micelles show high pH sensitivity in terms of toxicity. From pH 8.0 to 7.0 the toxicity is minimal due to shielding by pH sensitive sulfonamide polymer. The toxicity between pH 6.8 and 6.0 is high, comparable to free DOX. This trend presents a strong case for the pH sensitive biodegradable polymer that is able to protect the DOX loaded TAT-micelles at physiological pH and as the pH decreases to 6.8 the polymer is able to detach from the TAT-micelle. Upon detachment the TAT-micelle is able to produce the desired toxicity.

CONCLUSION

This paper describes a carrier system that not only modifies non specific TAT, but also presents an ultra pH sensitive biodegradable polymer. The carrier system could be used to effectively target tumor areas with an acidic profile. The designed biodegradable polymer was able to effectively shield the TAT-micelle system at normal pH and expose the micelles at lower acidic tumor pH. The biodegradable polymer showed resistance to degradation when complexed and rapid degradation in its native state. This carrier system brings us a step closer in our endeavor to a safe universal targeting system for acidic solid tumors.

ACKNOWLEDGMENTS

The authors wish to thank the Core Facilities at the University of Utah for use of the Mass and NMR spectroscopy and flow cytometer. This work was supported by NIH CA122356.

REFERENCES

1. E. S. Lee, K. Na, and Y. H. Bae. Polymeric micelle for tumor pH and folate-mediated targeting. *J. Control. Release.* **91**:103–113 (2003).
2. S. K. Han, K. Na, and Y. H. Bae. Sulfonamide based pH-sensitive polymeric micelles: physicochemical characteristics and pH-dependent aggregation. *Colloids Surf., A Physicochem. Eng. Asp.* **214**:49–59 (2003).
3. D. E. Discher and A. Eisenberg. Polymer vesicles. *Science* **297**:967–973 (2002).
4. F. Ahmed and D. E. Discher. Self-porating polymersomes of PEG-PLA and PEG-PCL: hydrolysis-triggered controlled release vesicles. *J. Control. Release* **96**:37–53 (2004).
5. I. Bala, S. Hariharan, and M. N. Kumar. PLGA nanoparticles in drug delivery: the state of the art. *Crit. Rev. Ther. Drug Carr. Syst.* **21**:387–422 (2004).
6. J. Panyam and V. Labhasetwar. Biodegradable nanoparticles for drug and gene delivery to cells and tissue. *Adv. Drug Deliv. Rev.* **55**:329–347 (2003).
7. M. Yokoyama, G. S. Kwon, T. Okano, Y. Sakurai, T. Seto, and K. Kataoka. Preparation of micelle-forming polymer–drug conjugates. *Bioconjug. Chem.* **3**:295–301 (1992).
8. K. Na, V. A. Sethuraman, and Y. H. Bae. Stimuli-sensitive polymeric micelles as anticancer drug carriers. *Anticancer Agents Med. Chem.* **6**:525–535 (2006).
9. S. R. Croy and G. S. Kwon. Polymeric micelles for drug delivery. *Curr. Pharm. Des.* **12**:4669–4684 (2006).
10. R. Kim. Recent advances in understanding the cell death pathways activated by anticancer therapy. *Cancer* **103**:1551–1560 (2005).
11. N. R. Wardwell and P. P. Massion. Novel strategies for the early detection and prevention of lung cancer. *Semin. Oncol.* **32**:259–268 (2005).
12. T. Minko, S. S. Dharap, R. I. Pakunlu, and Y. Wang. Molecular targeting of drug delivery systems to cancer. *Current Drug Targets* **5**:389–406 (2004).
13. M. Richter and H. Zhang. Receptor-targeted cancer therapy. *DNA Cell Biol.* **24**:271–282 (2005).
14. C. I. Spiridon, S. Guinn, and E. S. Vitetta. A comparison of the *in vitro* and *in vivo* activities of IgG and F(ab′)2 fragments of a mixture of three monoclonal anti-Her-2 antibodies. *Clin. Cancer Res.* **10**:3542–3551 (2004).
15. S. P. Vyas, A. Singh, and V. Sihorkar. Ligand–receptor-mediated drug delivery: an emerging paradigm in cellular drug targeting. *Crit. Rev. Ther. Drug Carr. Syst.* **18**:1–76 (2001).
16. V. A. Sethuraman and Y. H. Bae. TAT peptide-based micelle system for potential active targeting of anti-cancer agents to acidic solid tumors. *J. Control. Release* **118**:216–224 (2006).
17. R. J. Christie and D. W. Grainger. Design strategies to improve soluble macromolecular delivery constructs. *Adv. Drug Deliv. Rev.* **55**:421–437 (2003).
18. M. Meyer and E. Wagner. pH-responsive shielding of non-viral gene vectors. *Exp. Opin. Drug Deliv.* **3**:563–571 (2006).
19. A. Nori, K. D. Jensen, M. Tijerina, P. Kopeckova, and J. Kopecek. Subcellular trafficking of HPMA copolymer-Tat conjugates in human ovarian carcinoma cells. *J. Control. Release* **91**:53–59 (2003).
20. L. Hyndman, J. L. Lemoine, L. Huang, D. J. Porteous, A. C. Boyd, and X. Nan. HIV-1 Tat protein transduction domain peptide facilitates gene transfer in combination with cationic liposomes. *J. Control. Release* **99**:435–444 (2004).
21. S. Pujals, J. Fernandez-Carneado, C. Lopez-Iglesias, M. J. Kogan, and E. Giralt. Mechanistic aspects of CPP-mediated intracellular drug delivery: relevance of CPP self-assembly. *Biochim. Biophys. Acta* **1758**:264–279 (2006).
22. A. S. Ojugo, P. M. McSheehy, D. J. McIntyre, C. McCoy, M. Stubbs, M. O. Leach, I. R. Judson, and J. R. Griffiths. Measurement of the extracellular pH of solid tumours in mice by magnetic resonance spectroscopy: a comparison of exogenous (19)F and (31)P probes. *NMR Biomed.* **12**:495–504 (1999).
23. M. Stubbs, P. M. McSheehy, J. R. Griffiths, and C. L. Bashford. Causes and consequences of tumour acidity and implications for treatment. *Mol. Med. Today* **6**:15–19 (2000).

24. W. Yu, K. F. Pirollo, A. Rait, B. Yu, L. M. Xiang, W. Q. Huang, Q. Zhou, G. Ertem, and E. H. Chang. A sterically stabilized immunolipoplex for systemic administration of a therapeutic gene. *Gene. Ther.* **11**:1434–1440 (2004).
25. G. M. Kim, Y. H. Bae, and W. H. Jo. pH-induced micelle formation of poly(histidine-co-phenylalanine)-block-poly(ethylene glycol) in aqueous media. *Macromol. Biosci.* **5**:1118–1124 (2005).
26. S. I. Kang and Y. H. Bae. pH-induced volume-phase transition of hydrogels containing sulfonamide side group by reversible crystal formation. *Macromolecules* **34**:8173–8178 (2001).
27. S. I. Kang and Y. H. Bae. pH-induced solubility transition of sulfonamide-based polymers. *J. Control. Release* **80**:145–155 (2002).
28. S. I. Kang, K. Na, and Y. H. Bae. Sulfonamide-containing polymers: a new class of pH-sensitive polymers and gels. *Macromol. Symp.* **172**:149–156 (2001).
29. Y. Zong, X. Wang, K. C. Goodrich, A. M. Mohs, D. L. Parker, and Z. R. Lu. Contrast-enhanced MRI with new biodegradable macromolecular Gd(III) complexes in tumor-bearing mice. *Magn. Reson. Med.* **53**:835–842 (2005).
30. A. Lucke, J. Tessmar, E. Schnell, G. Schmeer, and A. Gopferich. Biodegradable poly(D,L-lactic acid)-poly(ethylene glycol)-monomethyl ether diblock copolymers: structures and surface properties relevant to their use as biomaterials. *Biomaterials* **21**:2361–2370 (2000).
31. K. Kataoka, A. Harada, and Y. Nagasaki. Block copolymer micelles for drug delivery: design, characterization and biological significance. *Adv. Drug Deliv. Rev.* **47**:113–131 (2001).
32. V. A. Sethuraman and Y. H. Bae. TAT peptide-based micelle system for potential active targeting of anti-cancer agents to acidic solid tumors. *J. Control. Release* **118**:216–224 (2007).
33. T. L. Kaneshiro, T. Ke, E. K. Jeong, D. L. Parker, and Z. R. Lu. Gd-DTPA L-cystine bisamide copolymers as novel biodegradable macromolecular contrast agents for MR blood pool imaging. *Pharm. Res.* **23**:1285–1294 (2006).
34. V. A. Sethuraman, K. Na, and Y. H. Bae. pH-responsive sulfonamide/PEI system for tumor specific gene delivery: an *in vitro* study. *Biomacromolecules* **7**:64–70 (2006).
35. S. I. Kang and Y. H. Bae. A sulfonamide based glucose-responsive hydrogel with covalently immobilized glucose oxidase and catalase. *J. Control. Release* **86**:115–121 (2003).
36. D. C. Bibby, N. M. Davies, and I. G. Tucker. Poly(acrylic acid) microspheres containing beta-cyclodextrin: loading and *in vitro* release of two dyes. *Int. J. Pharm.* **187**:243–250 (1999).
37. C. Ramkissoon-Ganorkar, F. Liu, M. Baudys, and S. W. Kim. Modulating insulin-release profile from pH/thermosensitive polymeric beads through polymer molecular weight. *J. Control. Release* **59**:287–298 (1999).
38. N. Raghunand, R. A. Gatenby, and R. J. Gillies. Microenvironmental and cellular consequences of altered blood flow in tumours. *Br. J. Radiol.* **76** Spec No 1: S11–S22 (2003).
39. X. L. Yang and A. H. Wang. Structural studies of atom-specific anticancer drugs acting on DNA. *Pharmacol. Ther.* **83**:181–215 (1999).